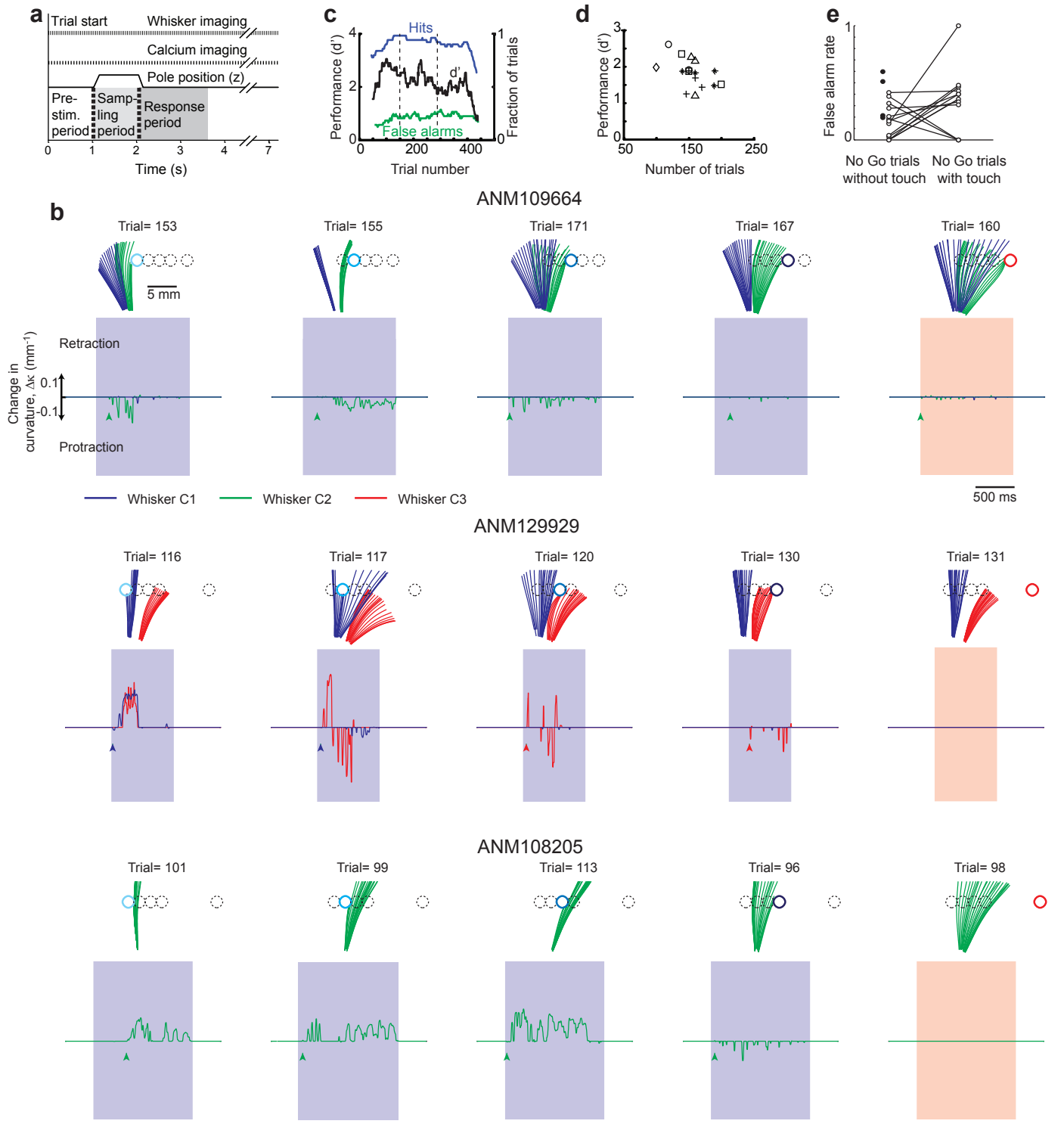

Petreanu et al.
Supplementary Figure 1

Supplementary Figure 1 | **Object localization behavior**. **a**, Temporal structure of the object localization task. The pole comes within reach during the sampling period (between vertical dashed lines). **b**, Whisking behavior over five trials (columns) for three animals (rows). Colored bars correspond to the sampling period (blue, Go; red, No Go). The pole location is indicated by a solid circle (dashed circles correspond to other object locations used during the session). For each trial, tracked whiskers are shown overlaid for the 40 milliseconds prior to first touch. When no touch was present (No Go trials; ANM129929 and ANM108205) 40 milliseconds prior to the pole coming within reach are shown. The traces represent curvature changes due to forces exerted by the object on the whisker (positive, retraction forces; negative, protraction forces). Colors correspond to different individual whiskers (red, C3; green, C2; blue, C1). The trials were consecutive sets, except that repeated object locations were removed. Arrowheads indicate first touch. **c**, Behavioral performance during one example imaging session (left axis, *d'*; right axis, fraction of correct Go trials (Hits) and incorrect No Go trials (False alarms). Vertical dashed lines indicate changes in imaging location. **d**, Behavioral data for all imaging sessions. Symbols indicate different animals. **e**, False alarm rate as a function of touch. In some behavioral sessions false alarm rate increased with touch. Solid circles, sessions without touches in No Go trials.

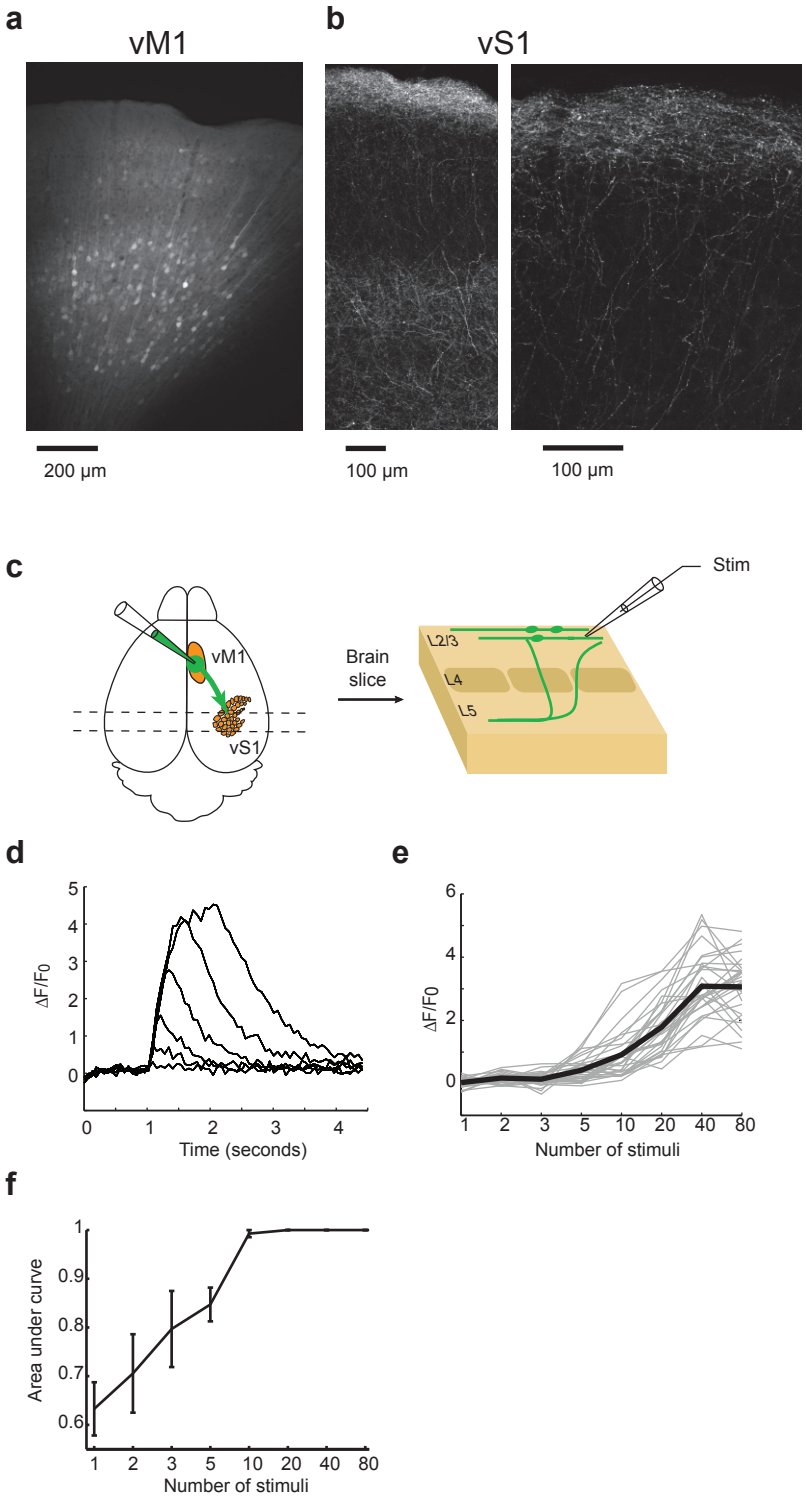

Petreanu et al.
Supplementary Figure 2

Supplementary Figure 2 | GCaMP3 characterization in axons in brain slices. **a**, Infection site in vM1 showing GCaMP3-expressing neurons in L2/3 and L5. **b**, GCaMP3-expressing axons in vS1.Note the high density of axons in layer 1, and to a lesser extent in L5. Right, blow-up showing axons in L1.**c**, Schematic of *in vivo* infection and brain slice. **d**, Fluorescence changes in response to trains of action potentials (83 Hz; 3, 5, 10, 20, 40, 80 APs; mean of 32 ROIs). **e**, Peak fluorescence change as a function of the number of action potentials (n = 32 variscosities; 2 mice). Similar results were obtained in thalamocortical slices (data not shown). **f**, Detection analysis. The plot shows the area under the ROC curve as a function of action potentials.

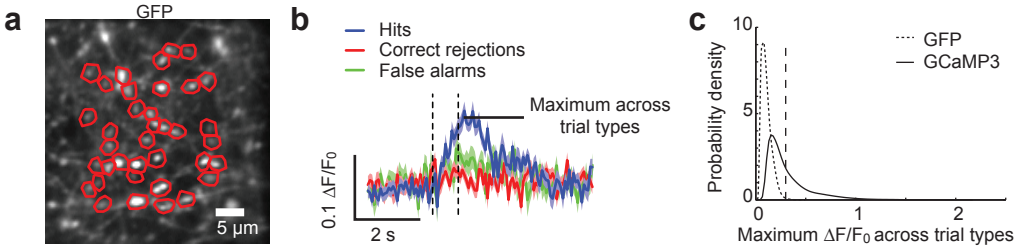

Petreanu et al.
Supplementary Figure 3

Supplementary Figure 3 | Control experiments with GFP-expressing axons to evaluate possible motion artifacts. Imaging and analysis were performed as with GCaMP3-labeled axons. **a,** Field of view showing ROIs surrounding individual GFP-positive varicosities. **b,** Movement-induced changes in fluorescence for one ROI averaged for different trial types (blue, Hits; red, Correct rejections; green, False alarms). **c,** Distribution of peak amplitudes of the fluorescence changes ($\Delta F/F$) for GFP-labeled varicosities (dotted line) and GCaMP3-labeled varicosities (solid line) (GFP, 108 ROIs, 3 animals, GCaMP3, 917 ROIs, 6 animals). The vertical dashed line corresponds to $\Delta F/F_0 = 0.3$, the threshold used for scoring a varicosity as 'active' in the GCaMP3 data. At most 1 % of the active varicosities could have been scored as active based on movement artifacts.

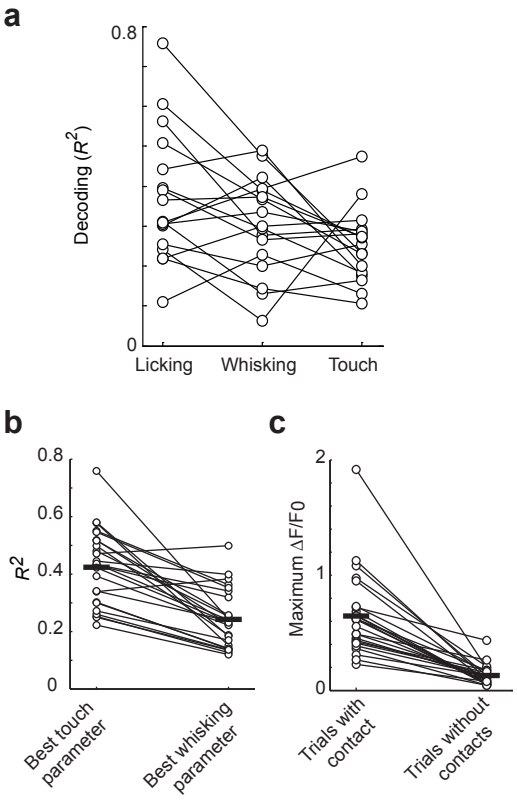

Petreanu et al.
Supplementary Figure 4

Supplementary Figure 4 | Decoding of behavioral variables based on populations and single axons. a, Decoding behavioral features based on activity in populations of axons. Correlation coefficients between the Random Forests model and different behavioral features. Each line corresponds to one field of view. Each field of view carries significant information about all measured behavioral variables, beyond what is expected based on trial averages ($p < 0.001$; bootstrap on trial-shuffled data). **b-c,** Additional analysis of touch-related axons. **b,** Most touch-related axons decoded touch forces better than whisking parameters. Note the two exceptions for which correlation with whisking was higher than with touch: For these axons touch forces were highly correlated with whisking, but activity was much lower in whisking trials without touch (panel c) and the axons were thus classified as touch-related. Horizontal bars, average. **c,** Touch-related axons were more active in trials with touch than without touch. Horizontal bars, average.

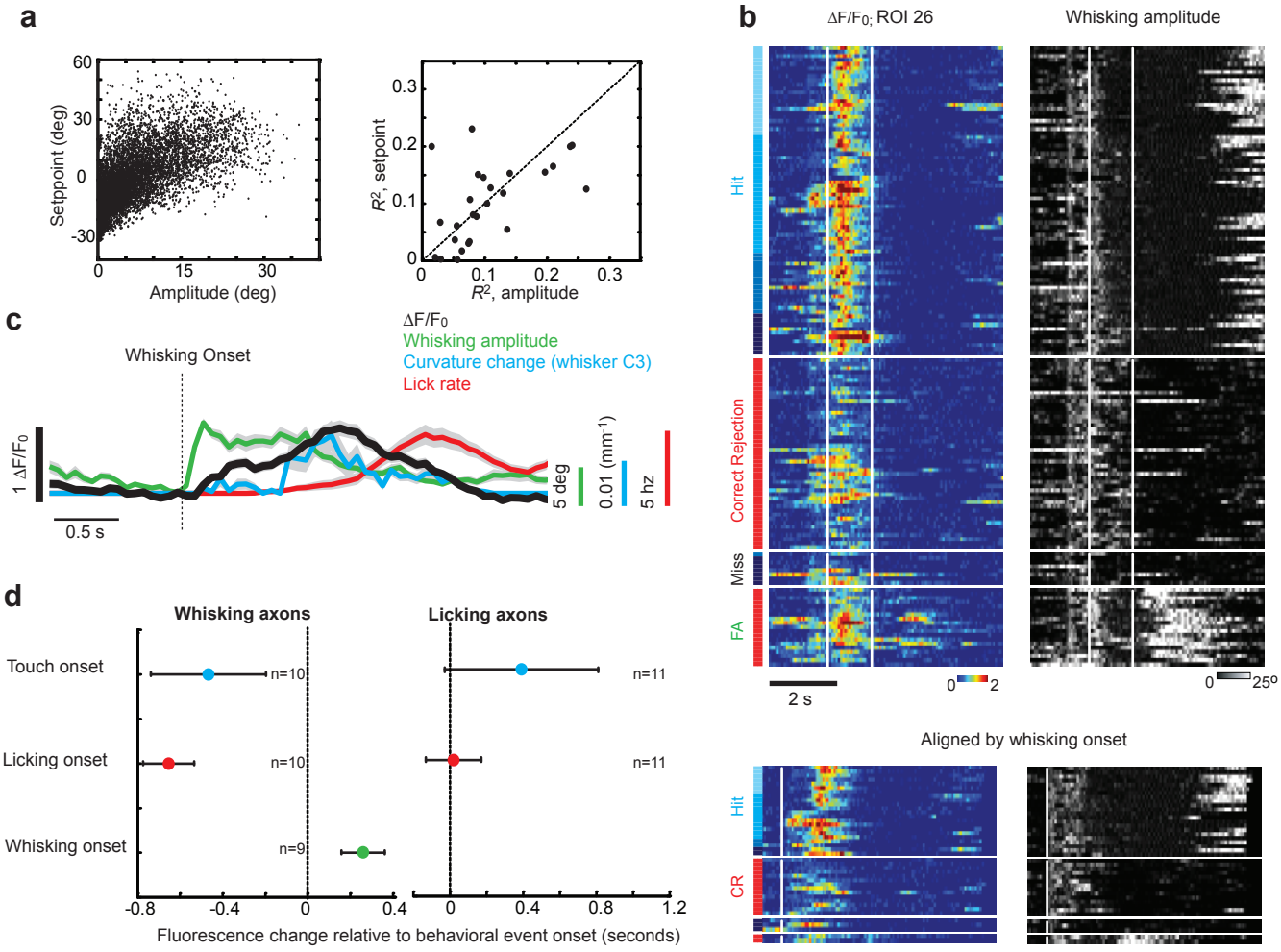

Petreanu et al.
Supplementary Figure 5

Supplementary Figure 5 | Further characterization of different axonal activity patterns. **a**, Left, correlation between whisking setpoint and whisking amplitude (one behavioral session). Each point corresponds to the average setpoint and amplitude in one imaging frame (64 ms) (R^2 = 0.36, linear regression). Right, performance of the decoding of setpoint and amplitude from the activity of whisking-related axons. Each point corresponds to one whisking-related axon over one behavioral session. **b**, Top, activity of one whisking axon and whisking amplitude. Bottom, activity aligned to whisking onset for the subset of trials with a well-defined whisking onset. **c**, Behavioral variables and activity of whisking-related axons (black) aligned to whisking onset. Same axon as in b. **d**, Left, timing of activity in whisking-related axons to onset of different behavioral features. Activity started after whisking onset, but well before touch and licking onset. Right, same analysis for lick-related axons. Activity in these axons started after touch and was coincident with licking. This analysis was based on the subset of trials (for example, bottom trials in panel b) that showed a sharp onset of movement and axons that showed a sharp onset of activity.

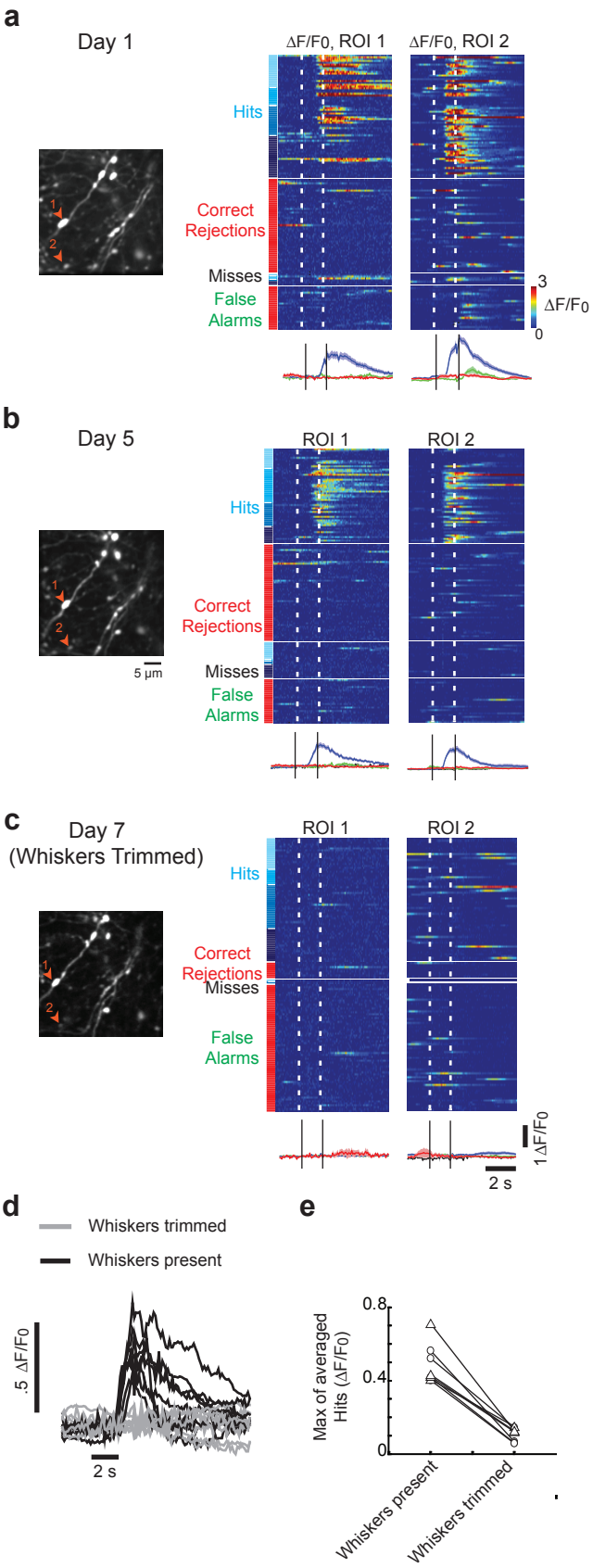

Petreanu et al.
Supplementary Figure 6

Supplementary Figure 6 | Chronic imaging. **a**, Left, image showing two varicosities marked by red arrow heads. Right, the corresponding fluorescence transients arranged by trial type. Bottom, PSTHs. **b**, Same varicosities four days later. The activity pattern was qualitatively stable. **c**, Immediately after whisker trimming, to abolish touch between the whiskers and the pole, touch-related activity disappeared. **d,** Touch-related axons were less active after whisker trimming so that touch did not occur (task-related whisking persisted, data not shown). **e**, Peak of PSTHs for Hits before and after trimming. Lines indicate the same ROI across days. Symbols, different animals.

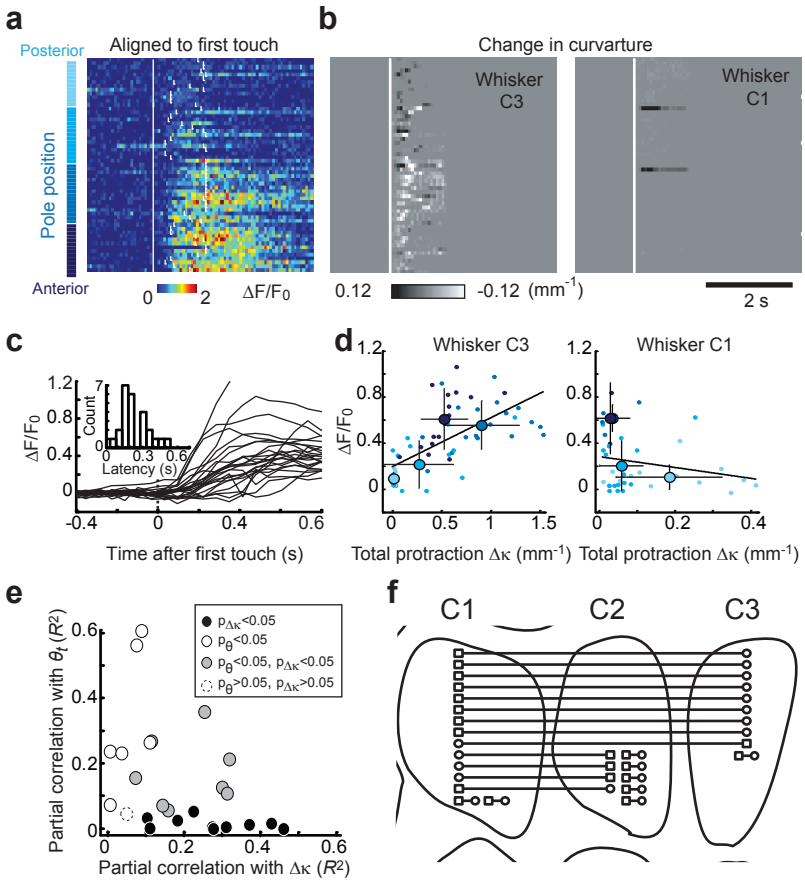

Petreanu et al.
Supplementary Figure 7

Supplementary Figure 7 | Low-level variables underlying object location-dependent activity. a, Activity of an example axon for different object locations (indicated by hues of blue on the left; cf Fig. 1b). Imaging was in the C1 barrel column. Activity was aligned to the first touch (vertical line). Ticks, last touch in each trial. Same example as Fig 4a. **b**, Curvature changes in whisker C3 (left) and C1 (Right) (whisker C2 was not present during this behavioral session) aligned to the first touch. Light, protractions; dark, retractions. **c**, Onset of activity from first touch for all axons showing object location-dependent activity (averaged across Hits; n=25). Inset, histogram of latencies (time from first touch to detectable deviation from baseline). **d**, Activity as a function of force ($\Delta\kappa$) on whisker C3 (left) and C1 (right). Total protraction $\Delta\kappa$ is the sum of all curvature changes across trial before the answer lick. **e**, We used partial correlation analysis to determine if forces on the whiskers ($\Delta\kappa$) can explain the variance in activity. Only trials with whisker contacts were included in the analysis. We correlated the fluorescence change (mean value from first contact to 1 second after the last contact) with the forces acting separately on each whisker (sum of all the protraction curvature changes, sum of retraction curvature changes, sum of all absolute value curvature changes, and mean curvature changes) while controlling for the azimuthal angle (θ) at contact. In a parallel analysis we allowed changes in θ at contact while controlling for curvature changes ($\Delta\kappa$). Solid circles, axons for which activity was explained by forces on one of the whiskers; open circles, activity explained by whisker position at touch (θ_t); grey circles, activity explained by both parameters. **f**, Correspondence between the dominant whisker (circle) and the anatomical principle whisker (square) of the imaged region of interest (n = 21). The dominant whisker was defined as the whisker whose forces or θ at contact resulted in the highest partial correlation. For many axons, $\Delta\kappa$ for one whisker dominated the variance of activity. However, the dominant whisker often (13/21) did not correspond to the principal whisker of the barrel column that contained the field of view. Sessions with only one whisker present or when the whisker corresponding to the imaged barrel was missing were excluded. Error bars, standard deviations.

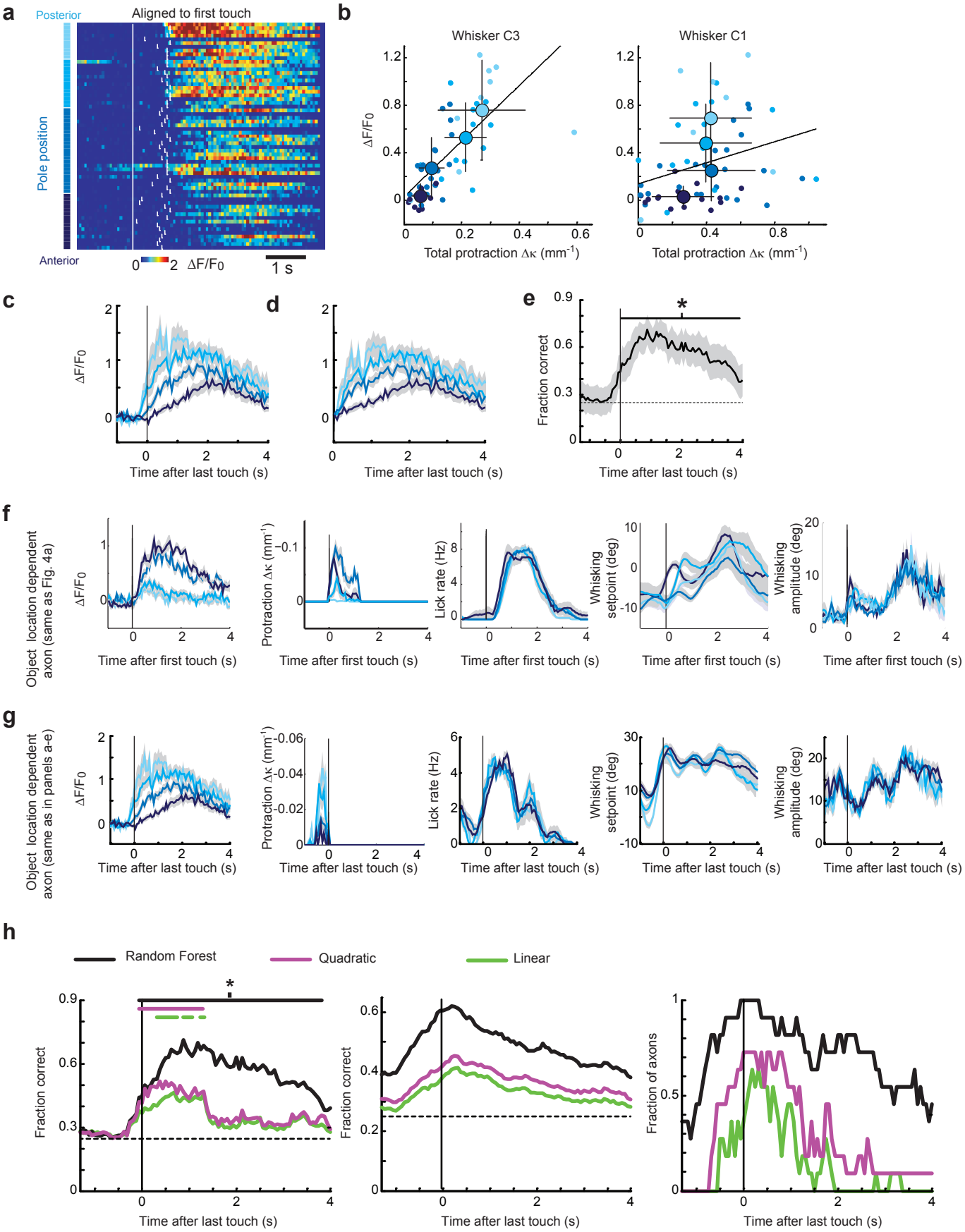

Petreanu et al.
Supplementary Figure 8

Supplementary Figure 8 | Further characterization of object location-dependent activity. **a,** Activity of one axon showing graded, object-location persistent activity for different object locations (indicated by hues of blue) during Hits, aligned to first touch. Ticks, last touch. Imaging was in the C3 barrel column. **b**, Activity as a function of forces on whisker C3 (left) and C1 (right) (whisker C2 was not present during this behavioral session). Error bars, standard deviations. **c**, Activity averaged across object locations, aligned to last touch (same axon as in a). **d**, Activity deconvolved to correct for the dynamics of calcium and GCaMP3 fluorescence (same axons as in c). **e**, The fraction of trials with correctly decoded object location as a function of time for the example axon shown in a. Dashed line, chance level (0.25, corresponding to four object locations). Horizontal line, time of significant decoding ($p < 0.05$). **f,g** Object-location dependent activity covaried with touch forces ($\Delta\kappa$) but not with motor behaviors. Averages at different object locations are indicated by different hues of blue;. Left two panels, object location-dependent activity (panel f: same data as in Fig. 4a-f, panel g: same data as in panels a-e). Right three panels, different behavioral features. Shading, s.e.m. **h**, Decoding of object location for different decoders (black, Random Forests; magenta, Quadratic; green, Linear). Left panel, fraction of trials decoded correctly by a single axon (same example as in a). Middle panel, decoding across the population of axons (corresponding to black line in Fig 4i). Right panel, fraction of axons decoding as a function of time (corresponding to red line in Fig. 4j).

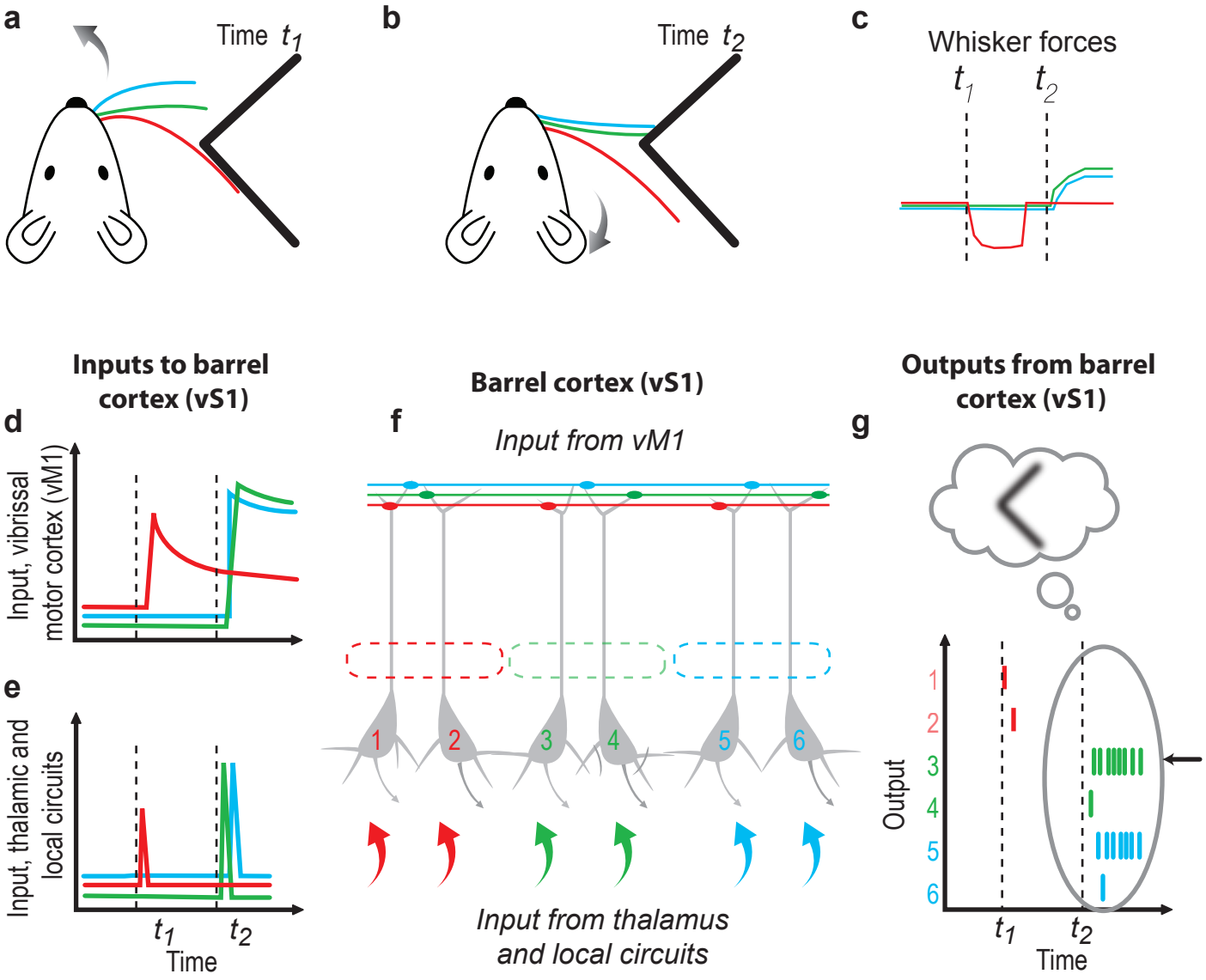

Petreanu et al.
Supplementary Figure 9

Supplementary Figure 9 | Schematic illustrating how somatosensory information might be integrated over space and time to produce a percept of object identity (i.e. a corner). **a**, Mouse protracting its whiskers against one wall of the corner at time t_1. **b**, , Mouse retracting its whiskers against the corner at t_2. Only two whiskers are touching. **c**, **d**,**e**, Inputs to barrel cortex. **d**, Different vM1 → vS1 axons showing persistent activity related to touch with the different whiskers. **e**, Phasic sensory input (from thalamus or local cortical neurons) in different barrel columns corresponding to individual whiskers. Note, the expected off response is omitted for simplicity. **f**, Confluence of top-down activity (memory related, from multiple whisker) and bottom-up activity (sensory) in L5 pyramidal neurons in the barrel cortex (although L5 neurons are illustrated here, the same picture holds for L2/3 cells). Synapses between vM1 axons and specific apical tufts are indicated by ellipses. **g**, Output from barrel cortex. Spiking output of an ensemble of vS1 neurons. Sensory input by itself causes single spikes, whereas coincident input into the apical tuft branches and basal dendrites is required to trigger burst firing. Neurons 3 and 5 receive input from a vM1 axon showing persistent activity signaling touch of the red whisker after t_1. After t_2 these neurons receive ascending touch-related input from the green and blue whiskers. Coincident input in the tuft and basal dendrites triggers bursts of action potentials signaling a sequence of touches, red followed by green and blue. Ensemble activity in vS1 (arrow) at t_2 could produce perception of a corner.